

# CFD Simulation Studies on Integrated Approach of Solar Chimney and Borehole Heat Exchanger for Building Space Conditioning

Shiv Lal<sup>1\*</sup>, Subhash Chand Kaushik<sup>2</sup>

RESEARCH ARTICLE

Received 12 May 2017; accepted after revision 19 August 2018

## Abstract

*In this communication, integrated approach of solar chimney and borehole heat exchanger has been studied by using computational fluid dynamics software. It is observed that, the room temperature can be maintained at 25-30 °C, at 4.9 ACH with this integrated approach in both peak summer and winter conditions. The cooling and heating effects are evaluated as 4.73-5.55 kW at 40 °C in summer and 8.27-10.56 kW at 5 °C in winter. The SC-BHE integrated system approach produced 21-37 % higher heating effect than the BHE alone system. In cooling mode SC fitted after the room in fluid circuit and it produces the induce effect for air suction from BHE along the air blower. So, integrated approach is a feasible solution for building space conditioning.*

## Keywords

*solar chimney, borehole heat exchanger, CFD, space conditioning*

## 1 Introduction

The utilization of solar energy for space heating is not a new concept though its applications increase day by day due to expensive conventional energy resources. Initially, the solar chimney was used for heating of buildings via passive mode. It was modified further for both applications in space heating and ventilation. In modified solar chimney, dampers were used for controlling the flow direction in MSC and it could be integrated with other passive system [1]. The numerous researchers and scientists have suggested that, the solar chimney is a very useful system for space heating and ventilation [2-6]. The indirect solar heat or ground heat can also use for heating and cooling of buildings. To extract the ground heat, two types of heat exchangers have been used viz. Horizontal ground coupled heat exchanger and vertical ground coupled heat exchanger. The borehole technology is simply known as vertical earth air heat exchanger and it gives better performance than horizontal.

The individual studies of solar chimney and borehole heat exchanger have been carried out by Lal et al. [7-10] both for experimentally and numerically. The individual elements validated through experimental study and stated that "no such experimental system have been found for validation of integrated approach". The results of our designed solar chimney and BHE integrated system found superior than the reported results in the literature. Lal et al. [11] studied the integrated approach of solar chimney and earth air tunnel heat exchanger and proposed the improved design and requirement of number of tunnels and solar chimney for particular heating and cooling load.

The integrated approach of SC and BHE is to be studied in this paper through CFD modelling and simulation. The velocity and temperature contour visualisation study is carried out. The feasibility study of SC-BHE integrated system is also carried out along with the numerical performance analysis.

## 2 Analysis of solar chimney-BHE integrated system

In this study the performance analysis of SC-BHE have been worked out with the velocity and temperature contour, and at different velocities, ambient temperature and solar radiation. The requirement of solar chimney and BHE for different

<sup>1</sup> Department of Mechanical Engineering,  
Rajasthan Technical University,  
Akelgarh, Rawatbhata Road Kota,  
PIN-324010, India

<sup>2</sup> Centre for Energy Studies,  
Indian Institute of Technology New Delhi,  
PIN-110016, India

\*Corresponding author, e-mail: [shivlal1@gmail.com](mailto:shivlal1@gmail.com)

cooling and heating load is also being estimated. A CFD model taking similar dimensions of the individual experimental system given in Lal et al [7, 9] is developed as below.

## 2.1 Mathematical Modelling

Navier-Stokes equation is used to govern the unsteady air flow / steady flow through the Borehole heat exchanger. For air flow through Borehole heat exchanger continuity, momentum and energy equations are given as follows is similar to [12]:

Continuity equation

$$\frac{\partial \rho}{\partial t} + \frac{\partial(\rho u)}{\partial x} + \frac{\partial(\rho v)}{\partial y} + \frac{\partial(\rho w)}{\partial z} = 0. \quad (1)$$

X-momentum equation

$$\frac{\partial(\rho u)}{\partial t} + \frac{\partial(\rho u^2)}{\partial x} + \frac{\partial(\rho uv)}{\partial y} + \frac{\partial(\rho uw)}{\partial z} = -\frac{\partial \rho}{\partial x} + \frac{1}{R_{ef}} \left[ \frac{\partial \tau_{xx}}{\partial x} + \frac{\partial \tau_{xy}}{\partial y} + \frac{\partial \tau_{xz}}{\partial z} \right]. \quad (2)$$

Y-momentum equation

$$\frac{\partial(\rho v)}{\partial t} + \frac{\partial(\rho uv)}{\partial x} + \frac{\partial(\rho v^2)}{\partial y} + \frac{\partial(\rho vw)}{\partial z} = -\frac{\partial \rho}{\partial y} + \frac{1}{R_{ef}} \left[ \frac{\partial \tau_{xy}}{\partial x} + \frac{\partial \tau_{yy}}{\partial y} + \frac{\partial \tau_{yz}}{\partial z} \right]. \quad (3)$$

Z-momentum equation

$$\frac{\partial(\rho w)}{\partial t} + \frac{\partial(\rho uw)}{\partial x} + \frac{\partial(\rho vw)}{\partial y} + \frac{\partial(\rho w^2)}{\partial z} = -\frac{\partial \rho}{\partial z} + \frac{1}{R_{ef}} \left[ \frac{\partial \tau_{xz}}{\partial x} + \frac{\partial \tau_{yz}}{\partial y} + \frac{\partial \tau_{zz}}{\partial z} \right]. \quad (4)$$

Energy equation

$$\begin{aligned} \frac{\partial(E_r)}{\partial t} + \frac{\partial(uE_r)}{\partial x} + \frac{\partial(vE_r)}{\partial y} + \frac{\partial(wE_r)}{\partial z} = & -\frac{\partial(up)}{\partial x} - \frac{\partial(vp)}{\partial y} \\ & - \frac{\partial(wp)}{\partial z} - \frac{1}{R_{ef} P_{rf}} \left[ \frac{\partial q_x}{\partial x} + \frac{\partial q_y}{\partial y} + \frac{\partial q_z}{\partial z} \right] \\ & + \frac{1}{R_{ef}} \left[ \frac{\partial(u\tau_{xx} + v\tau_{xy} + w\tau_{xz})}{\partial x} + \frac{\partial(u\tau_{xy} + v\tau_{yy} + w\tau_{yz})}{\partial y} \right. \\ & \left. + \frac{\partial(u\tau_{xz} + v\tau_{yz} + w\tau_{zz})}{\partial z} \right]. \end{aligned} \quad (5)$$

Transport equations for turbulent kinetic energy ( $k$ ) and turbulent dissipation energy ( $\epsilon$ ) are given as follows:

$$\frac{\partial(\rho k)}{\partial t} + \frac{\partial(\rho k u_j)}{\partial x_j} = \frac{\partial}{\partial x_j} \left[ \left( \mu + \frac{\mu_t}{\sigma_k} \right) \frac{\partial k}{\partial x_j} \right] + P_k + P_b - \rho \epsilon \quad (6)$$

$$\begin{aligned} -Y_M + S_k \\ \frac{\partial(\rho \epsilon)}{\partial t} + \frac{\partial(\rho \epsilon u_j)}{\partial x_j} = & \frac{\partial}{\partial x_j} \left[ \left( \mu + \frac{\mu_t}{\sigma_\epsilon} \right) \frac{\partial \epsilon}{\partial x_j} \right] + \rho C_1 S_\epsilon \\ & - \rho C_2 \frac{\epsilon^2}{k + \sqrt{v\epsilon}} - C_{3\epsilon} \frac{\epsilon}{k} P_b + S_\epsilon. \end{aligned} \quad (7)$$

Where, the model constants are  $P_k$  and  $P_b$  represent the generation of turbulent kinetic energy to the mean velocity gradients and buoyancy. Where,  $\epsilon$  is the dissipation,  $\mu_t$  is eddy viscosity and  $t$  represent the turbulent. Therefore the values of some constants are given as follows:

$$C_1 = 1.14, C_2 = 1.9, \sigma_k = 1.0, \sigma_\epsilon = 1.2.$$

We consider the Realizable k-epsilon model with the steady turbulent flow so that Reynolds-Averaged Navier-Stokes equations (RANS) are used for simulation with ( $k - \epsilon$ ) model. All the calculations were determined with the standard  $k - \epsilon$  model and the basic equation summarized as below.

## 2.2 Development of a CFD model of solar chimney-BHE integrated system

A two Dimensional geometry of solar chimney and BHE integrated system for space cooling is developed in design modular (DM) of ANSYS workbench (version 14.0). It is shown in Fig. 1. The dimension of the solar chimney and BHE are equal to the experimental system mentioned in Lal et al. [7, 9] respectively.

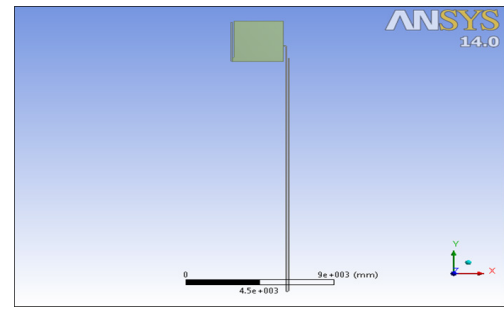


Fig. 1 SC-BHE integrated system for building space cooling

The sketch is transformed into three faces as air, glass and absorber surface, and seven edges as: inlet, outlet, pipe wall, outer glass surface, inner glass surface, inner absorber surface and outer absorber surface. After completion of nomenclature, the model is updated and edited in mesh software. The model is edited according to the requirement of mesh. The mesh has defined by different sizes in each room, pipe and chimney area and refined at the important edges. The quality of the mesh plays a direct role in the quality of the analysis, regardless of the flow solver. The final mesh for integrated approach of SC-BHE comprises 43975 elements and 39459 nodes. The mesh is well defined and uniform throughout the SC-BHE model other than nearby the surfaces.

A two dimensional model of SC-BHE integrated system for heating mode is also developed by using the above given procedure as shown in Fig. 2. The meshing of an integrated approach for space heating has been carried out using the above given procedure and it comprises 43846 elements and 39447 nodes. For simulation and modelling in Fluent, the mesh is updated and edited in Fluent.

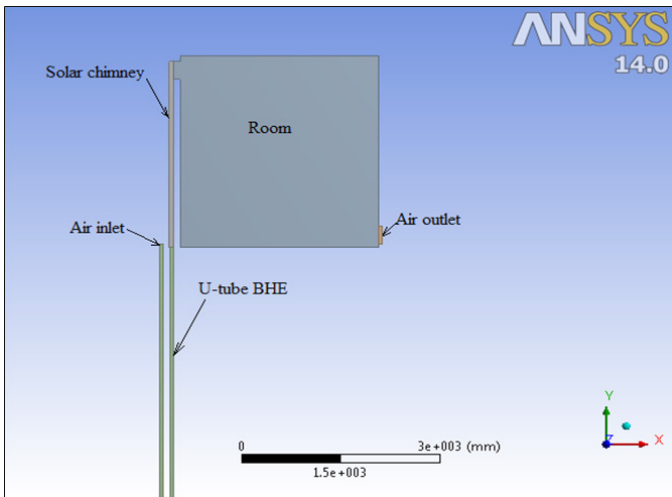


Fig. 2 SC-BHE integrated system for building space heating

### 2.3 Simulation of SC-BHE integrated system in FLUENT

To start the simulation in FLUENT, first we select the solutions strategy as: model selection, zones specification and boundary conditions. We have considered the steady ( $k - \epsilon$ ) realizable viscous flow model with standard wall function. The Discrete ordinate (DO) model has been used to account the radiation effect in solar chimney. The highly configured Work station has been used for simulation for reducing the simulation time and it is configured as: make-Dell precision T7400, 800 MHz multicore Intel Xeon processors (parallel processing), 64 GB RAM and a 1 TB HDD. The higher RAM with fast processor have used for reducing the simulation time. All boundary conditions have been set before starting the simulation. The simulation is initiated from the inlet point and completed up to the convergence at the end of flow. It will take time to simulate the model. After convergence, the results were obtained in the tabulated form as well as contour format. The properties of the input materials also defined in previous chapters.

## 3 Result and discussion

### 3.1 SC-BHE integrated system for space cooling and ventilation in buildings

#### 3.1.1 Effect of inlet velocity on building space cooling

The effect of mass flow rate at the outlet temperatures is shown in Fig. 3. The variable fluid velocity (2 to 8 m/s) have been taken at constant solar radiation as  $400 \text{ W/m}^2$  for this study. And it is seen that the solar chimney outlet temperature decreases and BHE & room temperature slightly increases with increases the mass flow rate of air. But after the optimum mass flow rate the air temperature at exit of BHE will be increased. It is found that the increment in room temperature due to increasing entropy is within the small range. It increases the total cooling effect due to increases mass flow rate. The solar

chimney effect is reducing when increases the air velocity in the system. So it can be beneficial in small variation only, because it is fixed after the room means in exit path of the system.

The velocity contour is shown in the Fig. 4. The colour visualization shows the velocity accounting in the flow path where red colour indicates the highest velocity at the end of BHE (Entering point to the room). The velocity inside the room is obviously constant at upper middle side and it is unstable at between the paths of BHE point to the chimney inlet point. The air velocity in the chimney again increases due to heating of air through solar radiation and generate stack effect.

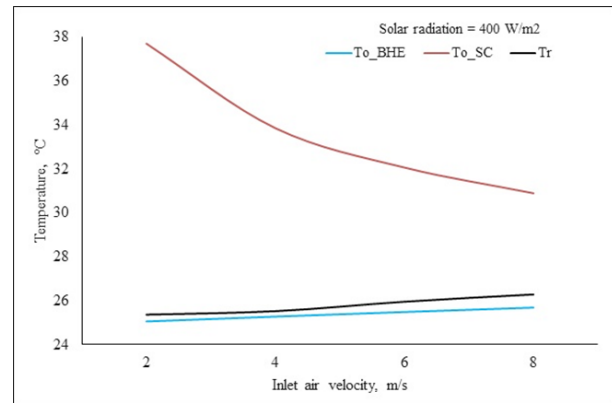


Fig. 3 Effect of inlet velocity on outlet temperatures

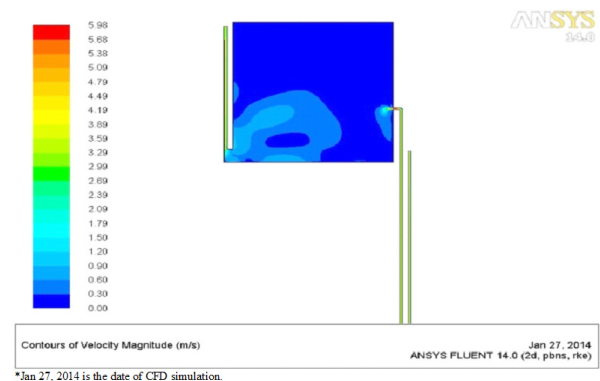


Fig. 4 Velocity contour of SC-BHE integrated system for space cooling

#### 3.1.2 Effect of Ambient temperature on building space cooling

The ambient temperature varying between  $35 \text{ }^\circ\text{C}$  to  $50 \text{ }^\circ\text{C}$  in the interval of  $5 \text{ }^\circ\text{C}$  at constant solar radiation, to study the effect of ambient temperature on building space cooling. The results of the simulation for this condition are shown in Fig. 5. BHE outlet and SC outlet temperature increases when increases the ambient temperature (inlet air temperature). The room temperature is found higher than BHE temperature and less than the SC temperature. The room temperature is observed between  $26\text{--}29 \text{ }^\circ\text{C}$  and it is a comfort zone as discussed in Fig. 1 for extreme temperatures. The SC-BHE cooling effect is obviously higher than SC-EATHE as proved in section 4 for same configuration EATHE and BHE.

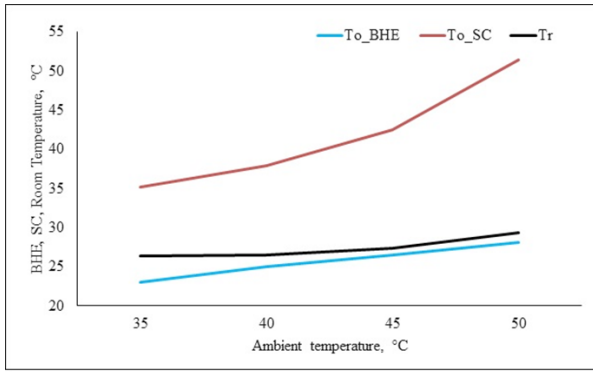


Fig. 5 Effect of ambient temperature on performance of integrated system in cooling mode.

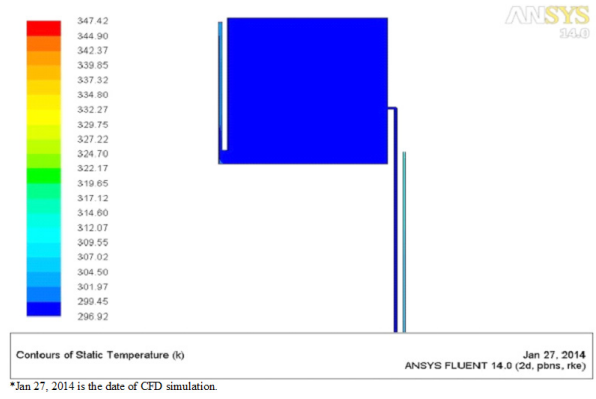


Fig. 6 Temperature contour of SC-BHE integrated system in cooling mode

### 3.1.3 Temperature distribution in the SC-BHE integrated system on building space cooling

The temperature decreases in BHE and increases in the solar chimney as shown in Fig. 6. The air temperature in the room observed uniform in all directions but air velocity doesn't found uniform. The temperature profile with the length of air path in the system is expressed in Fig. 7. It is found that, the minimum BHE outlet temperature (25.49 °C) observed slightly higher than the annual average temperature of the undisturbed earth (assumed 25 °C) from the simulation. The room temperature is maintained between 25.5-30 °C and it is in the comfort zone. The maximum cooling is due to BHE but a small effect is also presented by the SC on the cooling result.

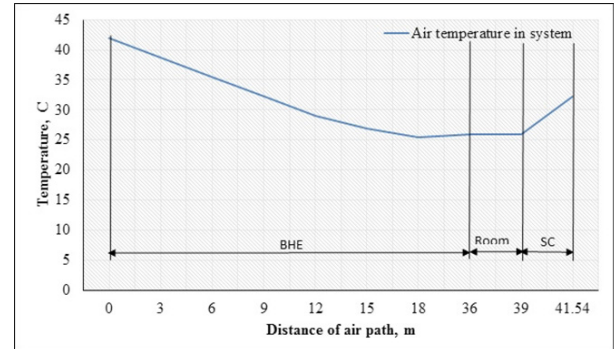


Fig. 7 Temperature variation in air flow path of SC-BHE integrated system in cooling mode

### 3.1.4 Cooling potential estimation the SC-BHE integrated system in cooling mode

The temperature variation with the solar radiation is expressed in Fig. 8. It is found that the room temperature is higher than BHE outlet temperature and lower than the SC temperature. The cooling potential of integrated approach is presented in Table 1. It is seen that the maximum cooling effect is observed due to BHE and a small cooling effect less than 70 W evaluated due to solar chimney. The diameter of U-tube in BHE is 2 inch and the depth of BHE is 60 feet in experimental. The depth of BHE will affect the cooling performance because the dampness of soil. The maximum and minimum cooling potential is to be estimated by 5.5 kW and 4.7 kW respectively. If the cooling demand increases by less than 70 W than only

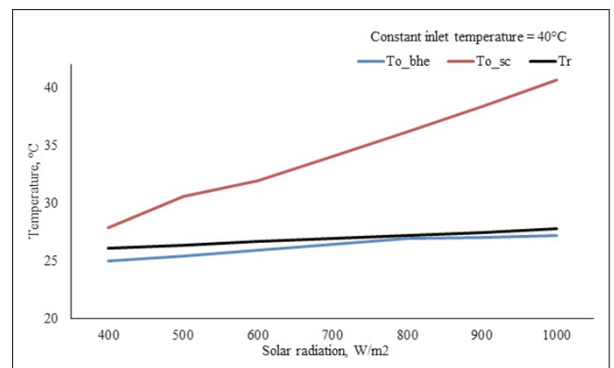


Fig. 8 Effect of solar radiation on of SC-BHE integrated system in cooling mode

one chimney is to be increased otherwise increasing the number of BHE to meet out the cooling demand.

Table 1 Performance of SC-BHE integrated system in cooling mode

S. No.	Solar radiation, W/m <sup>2</sup>	Velocities, m/s			Temperatures, °C			Cooling effect kW	ACH
		Vi	Vo-BHE	Vo-SC	Ti	To-BHE	To-SC		
1	400	14.8	17.66	14.55	40	24.97	27.88	5.55	4.9
2	500	14.8	22.05	14.65	40	25.38	30.58	5.39	4.9
3	600	14.8	22.07	14.76	40	25.96	31.94	5.18	4.9
4	700	14.8	22.07	14.84	40	26.42	34.02	5.01	4.9
5	800	14.8	22.07	14.92	40	26.92	36.12	4.83	4.9
6	900	14.8	22.07	14.99	40	27.05	38.4	4.78	4.9
7	1000	14.8	22.07	15.11	40	27.19	40.62	4.73	4.9

### 3.2 SC-BHE integrated system for space heating in buildings

#### 3.2.1 Effect of inlet velocity on building space heating

The effect of inlet velocity on SC-BHE integrated approach is shown in Fig. 9, it is found that SC, BHE and room temperature decreases with increase in air inlet velocity.

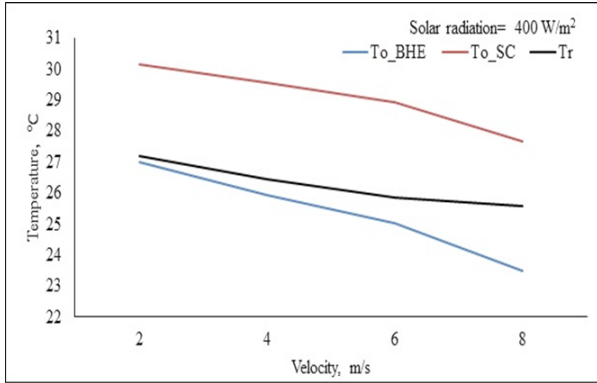


Fig. 9 Effect of inlet air velocity on performance of integrated approach in space heating mode.

#### 3.2.2 Effect of ambient air temperature on building space heating

The effect of ambient air temperature is expressed in the Fig. 10; it is simulated under constant solar radiation. It is seen that the space heating increases by increasing the ambient air temperature which is air inlet temperature. The room temperature is maintained between BHE outlet and solar chimney outlet temperatures, and it is found in comfort zone. The air temperature variation for throughout the air path is expressed in Fig. 11. The room temperature can be maintained in the comfort zone by this technology. Initial decrease in the room temperature can be attributed to the entrainment of hot supply air by the room air and this length of entrainment would be very short.

### 4 Heating potential estimation the SC-BHE integrated system

The effect of solar radiation on space heating due to SC-BHE integrated system is explained in Fig. 12, it is found that the chimney temperature increases due to solar radiation because solar chimney trapped the heat of solar radiation and result of that room temperature increases accordingly. The combined effect of solar chimney and borehole heat exchanger is found higher in heating mode than cooling mode. The solar chimney effect is fully utilised by the system in this time. If the heating demand increases we increases the number of solar chimney and reverse of that if cooling demand increases we increases the number of BHE, it is shown in Table 2. The main thing is to first estimate the cooling and heating demand in weather, and then optimisation of the system is possible. Maximum and

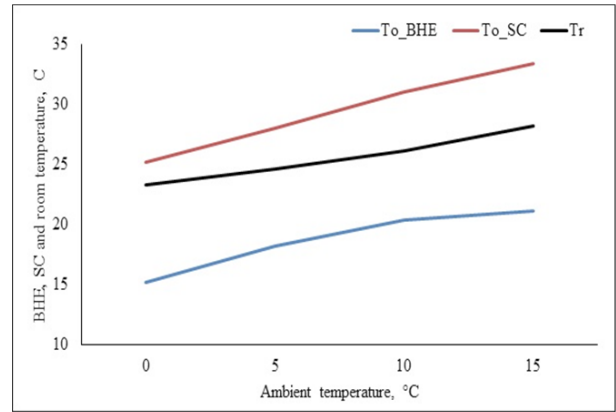


Fig. 10 Effect of ambient air temperature on space heating of building.

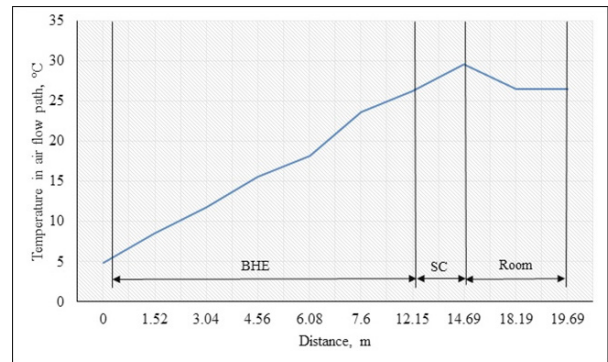


Fig. 11 Temperature variation in air flow path of SC-BHE integrated system in heating mode

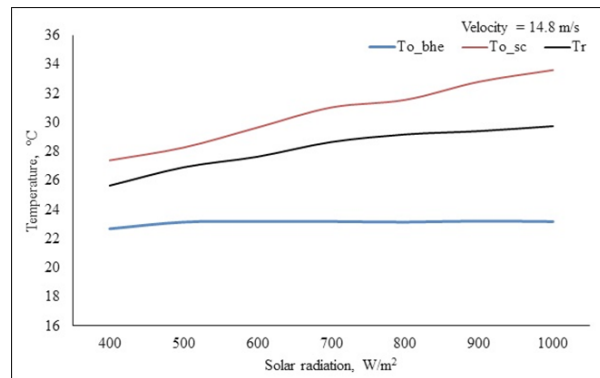


Fig. 12 Effect of solar radiation on system performance for space heating

minimum heating potential of a single SC-BHE integrated system is found to be as 10.56 kW and 8.27 kW respectively.

The SC-BHE integrated system approach produced 21-37 % higher heating effect than the BHE alone system. But it could not produce any significant cooling effect, because SC fitted after the room in fluid circuit and the air flow provided by air pump.

### 5 Conclusions

The solar chimney and BHE integrated approach has been studied for space cooling and heating of building. Two different CFD models have been constructed and simulated for variable solar radiation and variable ambient temperature.

**Table 2** Performance of SC-BHE integrated system for building space heating

S. No.	Solar radiation W/m <sup>2</sup>	Velocities, m/s			Temperatures, °C			Heating effect kW	ACH	Effect of SC %
		V <sub>i</sub>	V <sub>o</sub> -BHE	V <sub>o</sub> -SC	T <sub>i</sub>	T <sub>o</sub> -BHE	T <sub>o</sub> -SC			
1	400	14.8	16.55	14.48	5	22.69	27.4	8.27	4.9	21.03
2	500	14.8	16.55	14.48	5	23.15	28.28	8.59	4.9	22.04
3	600	14.8	16.55	14.48	5	23.2	29.66	9.11	4.9	26.20
4	700	14.8	16.55	14.48	5	23.19	31.04	9.62	4.9	30.15
5	800	14.8	16.55	14.48	5	23.15	31.56	9.81	4.9	31.66
6	900	14.8	16.55	14.48	5	23.22	32.81	10.27	4.9	34.48
7	1000	14.8	16.55	14.48	5	23.18	33.61	10.56	4.9	36.46

The performance of integrated approach has been studied for the requirement of solar chimney and BHE for specified cooling and heating demand. It is concluded that the integrated approach can be used for low temperature regions. The room temperature can be maintained at 25-30 °C, at 4.9 ACH by this integrated approach in peak summer and winter conditions. The cooling effect is evaluated by 4.73-5.55 kW at 40 °C ambient temperature and 400-1000 W/m<sup>2</sup> solar radiation. If the cooling demand increases more than this limit, at least two BHE will be required to meet out the demand. The space heating is evaluated as 8.27-10.56 kW at 5°C ambient temperature and 400-1000 W/m<sup>2</sup> solar radiation. The SC-BHE integrated system approach produced 21-37 % higher heating effect than the BHE alone system. But it could not produce any significant cooling effect, because SC fitted after the room in fluid circuit and the air flow provided by air pump.

### Nomenclature

$C$	Constant
$E$	Energy
$k$	Turbulent kinetic energy
$P_b$	generation of turbulence kinetic energy due to buoyancy
$P_k$	generation of turbulence kinetic energy due to the mean velocity gradients
$S_k$	modulus of the mean rate-of-strain tensor
$t$	time
$u$	Velocity component in x-direction
$v$	Velocity component in y-direction
$w$	Velocity component in z-direction
$Y_M$	Young's modulus
$\epsilon$	Turbulent Dissipation
$\mu$	Viscosity for steady flow
$\mu_t$	Eddy or turbulent viscosity
$\rho$	Density
$\tau$	Shear stress

### References

- [1] Lal, S., Kaushik, S. C., Bhargava, P. K. "A Study on Stack Ventilation System and Integrated Approaches." In: National Conference on Emerging Trends of Energy Conservation in Buildings, Central Building Research Institute (CBRI), Roorkee, India, Nov. 1-3, 2012. pp. 255-263.
- [2] Bansal, N. K., Mathur, R. Bhandari, M. S. "Solar chimney for enhanced stack ventilation." *Building and Environment*. 28(3), pp. 373-377. 1993. [https://doi.org/10.1016/0360-1323\(93\)90042-2](https://doi.org/10.1016/0360-1323(93)90042-2)
- [3] Khedari, J., Boonsri, B., Hirunlabh, J. "Ventilation impact of a solar chimney on indoor temperature fluctuation and air change in a school building." *Energy and Buildings*. 32(1), pp. 89-93. 2000. [https://doi.org/10.1016/S0378-7788\(99\)00042-0](https://doi.org/10.1016/S0378-7788(99)00042-0)
- [4] Ong, K. S., Chow C. C. "Performance of a solar chimney." *Solar Energy*. 74(1), pp. 1-17. 2003. [https://doi.org/10.1016/S0038-092X\(03\)00114-2](https://doi.org/10.1016/S0038-092X(03)00114-2)
- [5] Drori, U., Ziskind, G. "Induced ventilation of a one-story real-size building." *Energy and Buildings*. 36(9), pp. 881-890. 2004. <https://doi.org/10.1016/j.enbuild.2004.02.006>
- [6] Zhai, X. Q., Dai, Y. J., Wang, R. Z. "Comparison of heating and natural ventilation in a solar house induced by two roof solar collectors." *Applied Thermal Engineering*. 25(5-6), pp. 741-757. 2005. <https://doi.org/10.1016/j.applthermaleng.2004.08.001>
- [7] Lal, S., Kaushik, S. C., Bhargava, P. K., Balam, N. B. "Building Space Heating through Modified Trombe Wall: An experimental Study." In: International Conference on Smart Technologies for Mechanical Engineering, Delhi, India, Oct. 25-26, 2013. pp. 944-949.
- [8] Lal, S. "Experimental, CFD Simulation and Parametric Studies on Modified Solar Chimney for Building Ventilation." *Applied Solar Energy*. 50(1), pp. 37-43. 2014. <https://doi.org/10.3103/S0003701X14010125>
- [9] Lal, S., Balam, N. B., Jain, H. K. "Performance Evaluation, Energy Conservation Potential and Parametric Study of Borehole Heat Exchanger for Space Cooling in Building." *Journal of Renewable and Sustainable Energy*. 6(023123), pp. 1-12. 2014. <https://doi.org/10.1063/1.4872362>
- [10] Lal, S. "CFD simulation for the feasibility study of a modified solar chimney applied for building space heating." *World Journal of Modeling and Simulation*. 10(4), pp. 293-307. 2014.
- [11] Lal, S., Kaushik, S. C. "CFD Simulation Studies on Integrated Approach of Solar Chimney and Earth Air Tunnel Heat Exchanger for Building Space Conditioning." *International Journal of Economy, Energy and Environment*. 2(3), pp. 32-39. 2017. <https://doi.org/10.11648/j.ijeee.20170203.11>
- [12] "Mathematical modeling of RANS based turbulence k-epsilon model." [Online]. Available from: [http://www.cfd-online.com/Wiki/Standard\\_k-epsilon\\_model](http://www.cfd-online.com/Wiki/Standard_k-epsilon_model) [Accessed: 20th January 2013]